TITAN'S NEAR INFRARED ATMOSPHERIC TRANSMISSION AND SURFACE REFLECTANCE FROM THE CASSINI VISUAL AND INFRARED MAPPING SPECTROMETER.

P. Hayne[1,2] and T. B. McCord[2], J. W. Barnes[3], [1]University of California, Los Angeles (595 Charles Young Drive East, Los Angeles, CA 90095; phayne@ucla.edu), [2]The Bear Fight Center (Winthrop, WA), [3]University of Idaho (Moscow, ID).

1. Introduction: Titan's near infrared spectrum is dominated by absorption by atmospheric methane. Direct transmission of radiation from the surface through the full atmosphere is nearly zero, except in several methane "windows". In these narrow spectral regions, Titan's surface is visible, but our view is akin to peering through a dirty window pane, due to both N_2-induced pressure broadening of adjacent CH_4 lines and multiple scattering by stratospheric haze particles. Measured reflectance values in the methane windows are therefore only partially representative of true surface albedo.

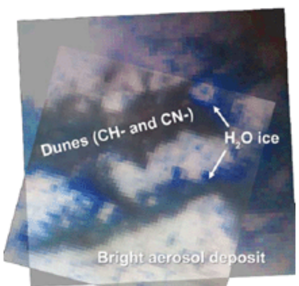

Figure 1: Titan surface materials

Using a simple radiative transfer model, we attempt a rudimentary correction to reflectance data from Cassini's Visual and Infrared Mapping Spectrometer (VIMS) [1]. We assume water ice in the Fensal-Aztlan region [2], and liquid ethane in Ontario Lacus [3] as calibration targets. We then assess the consequences for the presence of several other candidate surface materials. Of particular interest is the 2.7-2.8-µm "double window" (divided by an absorption of unknown origin), and the broad 5-µm window, which is least affected by scattering. Knowledge of atmospheric transmission in these two regions is especially crucial to interpreting spectra of two of Titan's most interesting surface features: Tui Regio and Hotei Regio.

2. Method: Incident monochromatic radiation at the surface is composed of direct and diffuse components:

$$I_{surf}^{\downarrow} = I_0 e^{-\tau/\mu_1} + \int_0^{\tau} J(\tau')d\tau'/\mu_1$$

where I_0 is the incident radiance at the top of the atmosphere, τ is the total optical depth at the surface, μ_1 is the cosine of the incidence angle, and J is a source function (which in general is also a function of I and μ). We assume isotropic scattering and approximate the source function as a function of optical depth alone:

$$\Gamma(\tau) = \int_0^{\tau} J(\tau')d\tau'$$

At the top of the atmosphere, the outgoing intensity is then

$$I_{top}^{\uparrow}/I_0 = A \cdot e^{-\tau(1/\mu_1 + 1/\mu_2)} + \beta \cdot \left(\frac{A}{\mu_1}e^{-\tau/\mu_1} + \frac{1}{\mu_2}\right) \quad (1)$$

where A is the (monochromatic) surface albedo, $\beta \equiv \Gamma/I_0$ is the ratio of the diffuse emergent intensity to the direct incident intensity at the top of the atmosphere, and μ_2 is the cosine of the emergence angle. To solve Equation (1), we make an initial guess $\bar{\tau}$ for the total optical depth, so that

$$\tau \approx -\mu' \ln\left[I/I_0 - \beta \cdot \left(\frac{A}{\mu_1} \cdot e^{-\bar{\tau}/\mu_1} + \frac{1}{\mu_2}\right)\right] + \mu' \ln A \quad (2)$$

where $\mu' \equiv 1/\left(1/\mu_1 + 1/\mu_2\right)$. Equation (2) converges rapidly to give an accurate estimate for $\tau(\lambda)$, given the surface albedo $A(\lambda)$ and an appropriate source function $\beta(\lambda)$. If there exists a calibration target of known albedo on Titan's surface, we can then calculate the atmospheric optical depth, and Equation (1) may then be used with the measured I/I_0 to find the albedo A for other areas of Titan.

3. Results:

Atmospheric Transmission: Mie theory suggests a scattering source function of the form $\beta(\lambda) = \sum_i a_i \lambda^{-i}$. We begin with this source function (choosing the a_i to match the observed diffuse reflectance function near the limb), then successively add terms representing multiple reflections between the surface and atmosphere. Due to the high albedo of the atmosphere, a feedback effect amplifies the surface

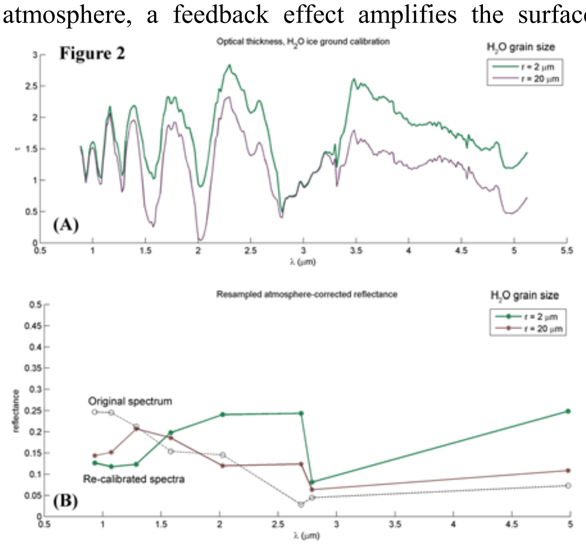

signal within the methane windows, especially at short wavlengths.

A suitable ground target is needed for the method to work. The Huygens probe sampled a single spot, with ambiguous compositional measurements [4]. However, Titan's bulk density and thermal evolution suggest a ~30 km shell of solid H_2O [5], which is consistent with the VIMS data for several regions [6, 7, 8]. A plausible model includes water-ice "bedrock" (**Figure 1**, blue unit) overlain by at least two other compositional units: "brown" ice/hydrocarbon dunes (e.g., "Fensal" region) and brighter, rough terrain (e.g., "Xanadu"). We take the pixels ($N \approx 20$) most spectrally similar to H_2O ice as a calibration target, using optical constants from [9]. **Figure 2a** shows the calculated atmospheric opacity and **2b** re-calibrated reflectance spectra of Tui Regio. Calibration using liquid ethane in the south polar lake Ontario Lacus, is in progress.

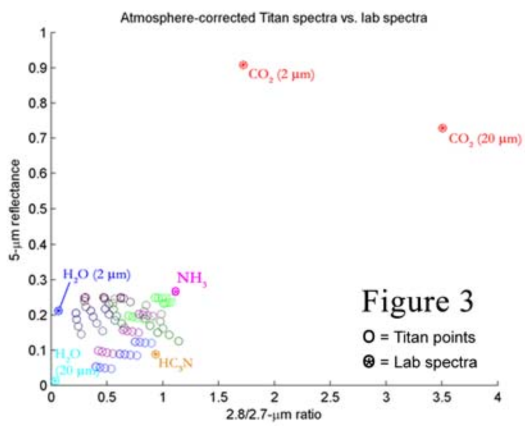

Surface Composition: McCord et al. (2008) suggested the presence of CO_2 frost to explain the brightest features on Titan, on the basis of three principal lines of evidence: (i) an absorption band near 4.9 μm, (ii) a high 5.0-μm reflectance, and (iii) a high 2.8/2.7-μm spectral contrast. R. Clark (2008, unpublished data) instead suggested cyanoacetylene, HC_3N, due to its better agreement with the 4.9-μm band position. Unlike CO_2, which has a strong 2.8/2.7-μm spectral contrast, HC_3N is nearly neutral in this region, as is ammonia ice, in apparent contradiction to the Titan data. Ammonia was suggested as the brightening agent behind a series of fluctuations at Hotei Regio, possibly implicating this spot as a cryovolcano [10]. Tui Regio is also a cryovolcano candidate [11].

Our results show that Tui Regio and Hotei Regio may simply be depleted in water ice relative to the rest of Titan. **Figure 3** is a scatterplot of 5-μm reflectance (I) versus 2.8/2.7-μm ratio (R) for the recalibrated spectra. The Titan points cluster around $I \approx 0.15$ and $R \approx 0.5 - 1.0$ (where 1.0 is a gray absorber). If our calibration target in Aztlan is indeed nearly pure H_2O ice, then atmospheric opacity is much higher at 2.7 μm than 2.8 μm, causing the observed spectral contrast > 1.0 in nearly all pixels. Since water ice of any grain size has a large blue slope in this spectral region, replacing it with a neutral component greatly enhances the observed 2.8/2.7-μm contrast. In this case, HC_3N and NH_3 are both consistent with Titan's brightest features.

4. Discussion: Enrichment in spectrally gray materials would explain Tui's and Hotei's high 2.8/2.7-μm contrast and high reflectance at 5.0 μm. HC_3N and NH_3 would be reasonable candidates, though NH_3 lacks the observed narrow 4.9-μm absorption. However, it is likely that our calibration target is not pure water ice, which would bring the corrected Titan points closer to CO_2 in Figure 3. Further, we may question whether the high 2.8/2.7-μm ratio originates in the atmosphere, rather than some ubiquitous surface material, e.g., CO_2. In fact, this ratio is observed to be proportional to the atmospheric path length (**Figure 4**), and is also observed at the tops of tropospheric clouds, which should be spectrally neutral in the near infrared. We therefore suggest that the 2.8-μm spectral contrast is largely atmospheric. While this analysis favors HC_3N and NH_3 over CO_2, the latter is not necessarily ruled out, since our basic assumption, i.e. that the VIMS "blue unit" is pure H_2O ice, is almost certainly inaccurate to some degree; the target could instead be mostly CO_2. A similar analysis using Ontario Lacus, will likely provide better constraints on Titan's atmospheric transmission in this key spectral region.

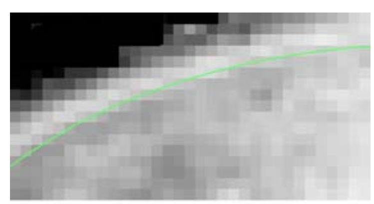

Figure 4: Limb 2.8/2.7-μm ratio

References: [1] Brown, R. H. et al. (2004) *Space Sci. Rev.* 115, pp. 111-168. [2] McCord, T. B. et al. (2006) *Planet. Space Sci.* 54, pp. 1524-1539. [3] Brown, R. H. et al. (2008) *Nature* 454, 607-610. [4] Niemann, H. B. et al. (2005) *Nature* 438, 779-784. [5] Grasset, O. et al. (2000) *Planet. Space Sci.* 48, 617–636. [6] Soderblom, L. A. et al. (2007) *Planet. Space Sci.* 55, 2025-2036. [7] McCord, T. B. et al. (2008) *Icarus* 194, 212-242. [8] Barnes, J. W. et al. (2007) *Icarus* 186, 242-258. [9] Hansen, G. B. (2008) Unpublished spectra. [10] Nelson et al. (2009), *Icarus*, in press. [11] Barnes, J. W. et al. (2006) *Geophys. Res. Lett.* 33, L16204.